

# Interesting behavior for filtration of macromolecules through EVAL membranes

T.-H. Young<sup>a,\*</sup>, L.-P. Cheng<sup>b</sup>, H.-Y. Lin<sup>a</sup>

<sup>a</sup>*Institute of Biomedical Engineering, College of Medicine and College of Engineering, National Taiwan University, Taipei, Taiwan*

<sup>b</sup>*Department of Chemical Engineering, Tamkang University, Taipei, Taiwan*

Received 19 October 1998; received in revised form 14 January 1999; accepted 11 February 1999

## Abstract

The objective of this article is to investigate the permeation characteristics of several polydispersed macromolecules through the asymmetric and the particulate poly (ethylene-co-vinyl alcohol) (EVAL) membranes. The solutes in examination include two nonionic solutes, dextran and polyethylene glycol (PEG), and one anionic solute, sodium polyacrylate (SPA). The ultrafiltration results indicate that the rejection coefficients increase monotonically with the molecular weights of test solutes permeating through the asymmetric EVAL membranes. This is consistent with the behavior of normal commercial ultrafiltration membranes. For the particulate membranes, the rejection curves show different trends. In most cases, there exist two local minima in the rejection curves, having the shape of “W”. This unusual behavior is found to be associated with the dual-pore character of the particulate membrane. To this context, a parallel composite membrane model is proposed to explain this specific rejection in terms of rejection coefficients for the small and the large pores. © 1999 Elsevier Science Ltd. All rights reserved.

*Key words:* EVAL; Asymmetric membranes; Particulate membranes

## 1. Introduction

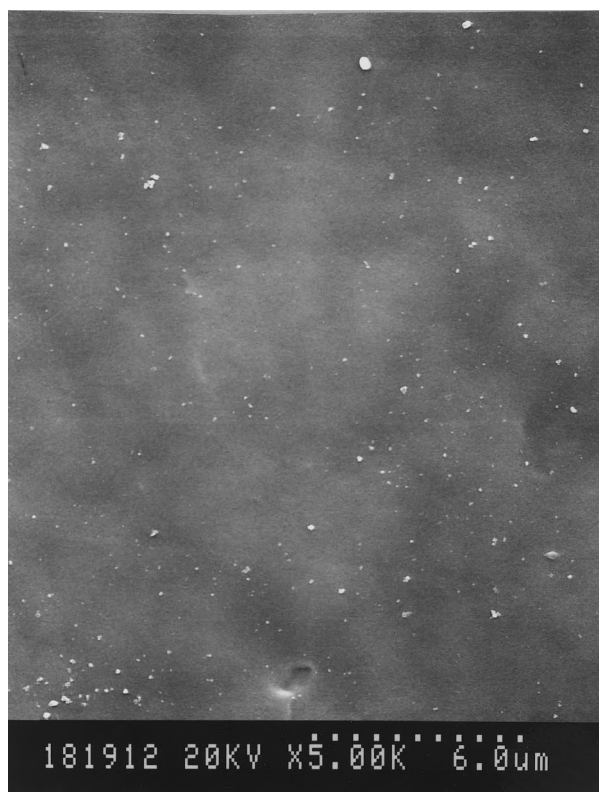
Since the development of asymmetric type membrane by Loeb and Sourirajan [1] in the 60th, the field of membrane science/technology has experienced a steady growth in many phases of separation processes. The asymmetrical membrane features a skin layer, which is generally very thin and tight, with pore size falling in the domain of submicron or less. This skin region functions as a selective barrier that separates the incoming chemical species through specific interaction or size exclusion mechanism. On the whole, the properties of the skin, such as the pore size, the compactness, the functional groups etc. dictate the areas of applications of the membrane (e.g. microfiltration, ultrafiltration, desalination, pervaporation, etc). Underneath the skin is a thick porous structure, which provides the membrane with adequate mechanical strength. This sublayer has large pores and sometimes finger-like macrovoids such that it offers little resistance and selectivity toward solute transport. In a previous article [2], we reported the dextran rejection characteristics both of the asymmetric and the particulate

poly (ethylene-co-vinyl alcohol) (EVAL) membranes. The particulate EVAL membrane is uniform and skinless composed of equal-sized spherical particles that pack into a bi-continuous porous structure. There are two types of pores in this membrane: small nano-order pores inside the EVAL particles and large micron-order continuous pores surrounding the particles. As both types of pores are available to the migration of solute molecules, the rejection behavior of this membrane differs markedly from ordinary ultrafiltration membranes, viz., small solute molecules tend to be rejected rather than large solute molecules [2].

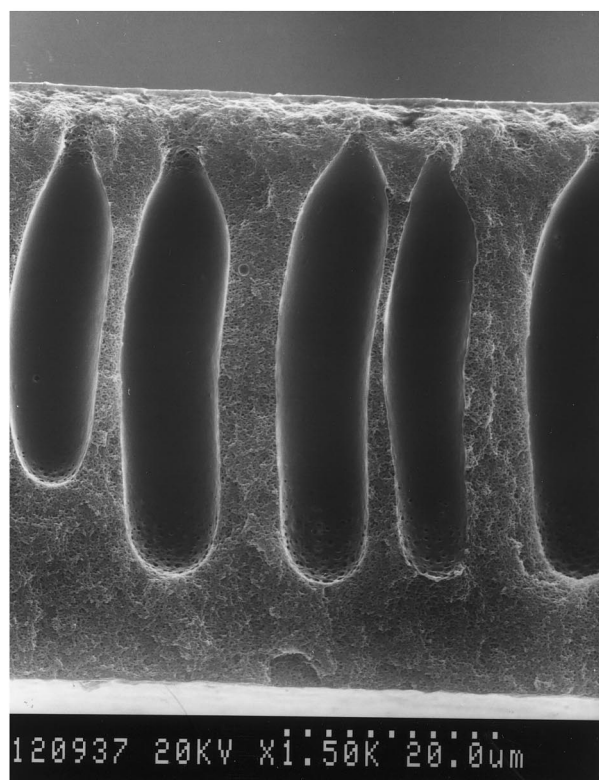
In the present article, we investigate further the morphology and its relation to ultrafiltration performance of asymmetric and particulate EVAL membranes. Two nonionic solute molecules, dextran and polyethylene glycol (PEG), and one anionic solute, sodium polyacrylate (SPA), of various molecular weights are employed. The rejection coefficients versus molecular weights of these solutes permeating through the particulate membrane demonstrate an unusual shape, “W”. Assuming that, during filtration, solute accumulation in the membrane is negligible and that steady state has been attained at the time when effluent samples are analyzed, we rationalize this “W-shape” rejection curve, in terms of rejection coefficients associated with transportation within the small and the large pores. These

\* Corresponding author. Tel.: +886-2-23970800 ext. 1455; fax: +886-2-23940049.

*E-mail address:* thyoung@ha.mc.ntu.edu.tw (T.-H. Young)



(a)



(b)

Fig. 1. SEM photomicrographs of an asymmetric EVAL membrane prepared by immersing a 25 wt.% dope solution in water: (a) top surface; (b) cross-section.

assumptions are justifiable due to the facts that low solute concentration with a vigorous agitation and a small transmembrane pressure are employed during the filtration process [2]. In addition, the effects of pressure on the rejection curves are also studied.

## 2. Experimental

### 2.1. Material

#### 2.1.1. Material for membrane formation

The membrane material studied in this work was EVAL copolymer containing ca. 56 mol% vinyl alcohol. The measured intrinsic viscosity was 0.87 dl/g, and  $M_{\eta} = 56,000$  g/mol [3]. Kuraray Co. Ltd., Japan kindly supplied this polymer. Dimethyl sulfoxide (DMSO) and 1-octanol (extra pure reagent grade, Nacalai Tesque, Kyoto, Japan) were used as received. Water was double distilled and de-ionized before used.

#### 2.1.2. Polymeric solutes for filtration

Three types of polymeric solutes were studied in this work. Dextrans with average molecular weights of 11.5, 41, 70 and 505 kDa were purchased from Sigma and a smaller dextran,  $M = 6$  kDa was purchased from Fluka. PEG with  $M = 2, 6, 20,$  and  $70$  kDa were obtained from Nacalai Tesque (Kyoto, Japan) and another PEG,  $M = 35$  kDa, was obtained from Fluka. SPAs with  $M = 2.1, 5.1, 20,$  and  $60$  kDa was obtained from Fluka.

### 2.2. Membrane preparation and characterization

Membranes were prepared using the direct immersion precipitation method. An appropriate amount of EVAL was dissolved in DMSO to form a 25 wt.% homogeneous dope solution. This solution was cast uniformly on a glass plate (the casting thickness was ca.  $100 \mu\text{m}$ ) using an auto-coater (KCC303, RK Print-Coat Instruments, UK) and then immersed directly in either water or 1-octanol bath to effect precipitation. The formed membrane was freeze-dried and examined with a scanning electron microscope (SEM, S-800, Hitachi).

### 2.3. Filtration

All filtration experiments were carried out at room temperature ( $20 \pm 3^\circ\text{C}$ ) and a constant transmembrane pressure, using a 25 mm diameter Amicon Stirred Ultrafiltration Cell (Model 8010) with a vigorous agitation (600 rpm) to minimize the effect of concentration polarization. Compressed nitrogen gas was used as the pressure source. The feed solutions (total concentration 1000 ppm) were prepared by dissolving pre-weighted quantities of powder solutes with a wide distributed molecular weights in distilled–deionized water. These solutions were agitated in a mixer for 24 h. to insure complete dissolution. Three

transmembrane pressures were employed, i.e. 0.25, 0.5 and 0.75 kgf/cm<sup>2</sup>. After the permeation flux reached a stable constant value (ca. 50 min. after operation), samples of filtrate were collected for subsequent chromatographic analysis. To check whether the membrane has any defect, a solution containing 100 ppm blue dextran was used as the feed. The average molecular weight of this blue dextran was 2000 kDa (Sigma). All tested membranes were found to reject the blue dextran.

#### 2.4. Chromatographic analysis

Dextran, PEG and SPA samples were analyzed by gel permeation chromatography (GPC, Waters) using a Phenomenex Bio-SEC-S4000 column (Phenomenex Corporation, USA). Deionized water was used as the mobile phase. The eluent flow rate was maintained at 1.0 ml/min using a SPECTROFLOW 400 (Applied Biosystem Corporation, USA). The refractive index detector in this system was Shodex RI SE-61 (Showa Denko Corporation, Japan). The retention time was related to the molecular weight using calibration curves constructed from respective polymer standards. The molecular weights of standards as quoted by the manufacturers were assumed to be correct.

### 3. Results and discussion

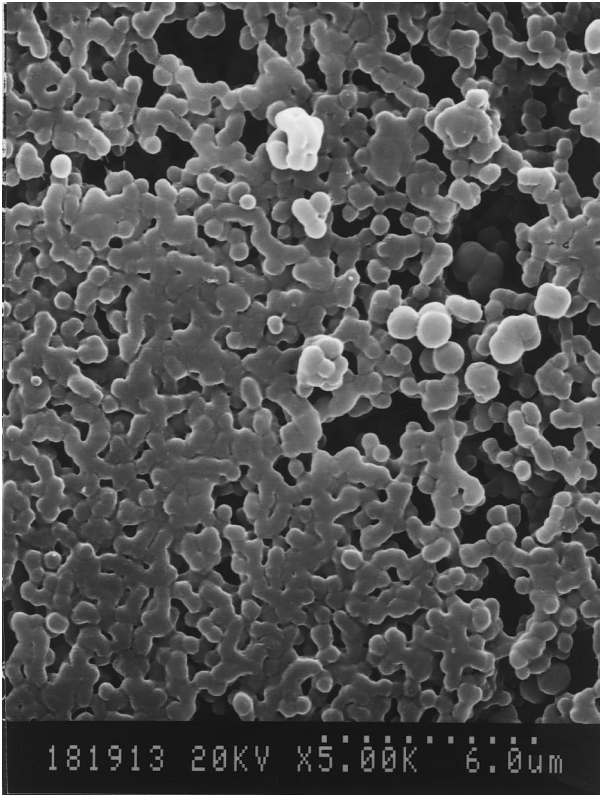
In Fig. 1, morphology of the membrane formed by immersing a 25 wt.% EVAL solution into a water bath is shown. This membrane exhibits an asymmetric structure consisting of a thin skin layer atop a thick porous layer that contains finger-like macrovoids extending into the bottom region of the membrane. The skin layer is dense and is thus responsible for the permeation (or rejection) of solutes, whereas the porous bulk acts simply as a mechanical support. The membrane formation mechanism has been discussed in a previous article [4]. In addition to the asymmetric morphology, EVAL membrane morphology can be tailored into a particulate one by precipitation in 1-octanol bath. The top surface and cross-section of such membrane are shown in Fig. 2. It appears that this membrane is uniform and skinless. The pores between EVAL particles interconnect into continuous yet tortuous channels. Young et al. have rationalized the formation mechanism for this structure [3,5].

Filtration of dextran, PEG and SPA are carried out both for the asymmetric and the particulate membranes. Concentrations of solute are measured at steady effluent flux; from which data the rejection behavior for filtration of macromolecules through EVAL membranes is calculated. Fig. 3 shows the relation between permeate flux and time for filtration of PEG through asymmetric and particulate EVAL membranes with the applied pressure of 0.75 kgf/cm<sup>2</sup>. This trend was also observed in the cases of other solute polymers at different pressures (not shown here). As the concentrations of polymer solutes for filtration were low

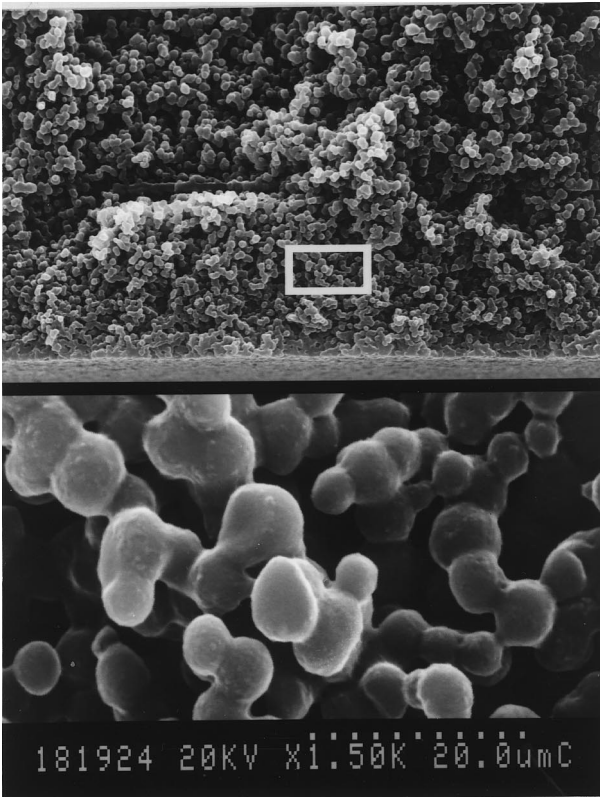
and with a vigorous agitation, the fluxes approached the pure water fluxes. (The pure water fluxes for asymmetric and particulate EVAL membranes at the applied pressure of 0.75 kgf/cm<sup>2</sup> were  $6.8 \times 10^{-6}$  and  $2.6 \times 10^{-6}$  m/s, respectively.) In particular, the declination of permeate flux during the transition time for the particulate membrane was relatively small and the flux remained essentially constant once a steady value was reached, suggesting that the concentration polarization was negligible for the time scale of our experiments. However, the effect of concentration polarization can be estimated by considering the mass transfer coefficient and the flow rates. In our previous publication [2], we have shown that the observed and actual sieving coefficients for dextran (13K) through asymmetric and particulate EVAL membranes at 0.25 kgf/cm<sup>2</sup> were essentially identical. This again indicated that the concentration polarization was insignificant and could be ignored.

Fig. 4 shows the results for filtration through asymmetric EVAL membranes in terms of rejection coefficients versus the molecular weight of different solute polymers (dextran, PEG and SPA). The operational pressure is 0.5 kgf/cm<sup>2</sup> in all cases. It can be observed that the rejection coefficients increase monotonically with the molecular weight of the solute, as in ordinary filtration processes. As asymmetric membranes have their effective rejections occurring in the skin, once a particle penetrates through this layer, it flows almost straight through the porous bulk. As a result, small molecules always have smaller rejection coefficients than large molecules. Fig. 4 indicates that the rejection coefficients of SPA are only somewhat larger than those of PEG and notably larger than those of dextran, for solutes of the same molecular weight. This trend is similar to the calibration curve of SPA, PEG and dextran in GPC (not shown here). The divergence is believed to be primarily due to the shape and size of randomly coiled macromolecules in water or/and the interaction of the macromolecules with membrane [6].

Likewise, SPA has the largest whereas dextran has the smallest rejection coefficients for filtration through particulate EVAL membranes, as shown in Fig. 5. These solute rejection curves, however, differ considerably from those for the asymmetric membranes. The rejection curves for dextran and SPA have the shape of “W” and for PEG, the curve exhibits a minimum. In the discussion that follows, we will first focus on the rejection behavior of dextran and SPA due to their analogous rejection pattern; as to PEG, the role of pressure is found to be important and will be discussed lastly. As shown in Fig. 5, the rejection curve for dextran consists of four sections. At first, the rejection coefficient decreases with increasing molecular weight (Section 1), then, it increases (Section 2) and then decreases again (Section 3). In other words, if there were concentration polarization in our experiments, increase rather than decrease of rejection with molecular weight would be observed. This confirms (although indirectly) that the concentration polarization was minor in our system. Finally,



(a)



(b)

Fig. 2. SEM photomicrographs of a particulate EVAL membrane prepared by immersing a 25 wt.% dope solution in 1-octanol: (a) top surface, (b) cross-section.

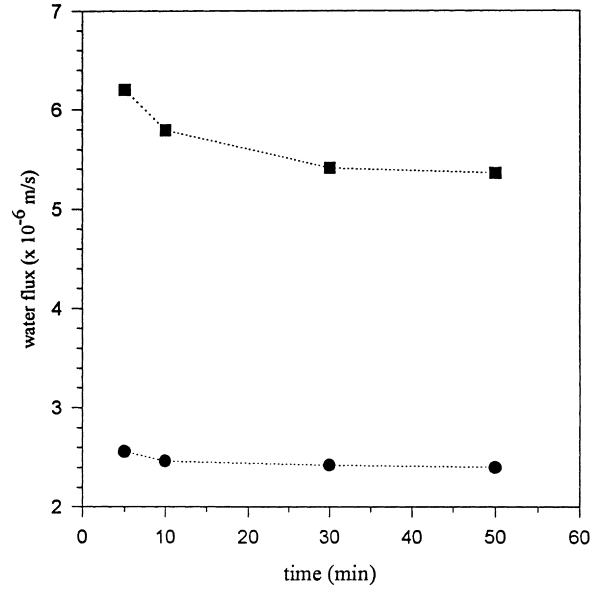


Fig. 3. Relation between permeate flux and time for filtration of PEG through asymmetric (●) and particulate (■) EVAL membranes with the applied pressure of 0.75 kgf/cm<sup>2</sup>.

the rejection coefficient undergoes a rapid increase to reach complete retention (Section 4). (Note: the particulate membranes reject blue dextrans with a molecular weight of 2000 kDa.) It has been demonstrated in a previous article that dextran molecules of different sizes permeate through the particulate membrane following different paths [2]. This

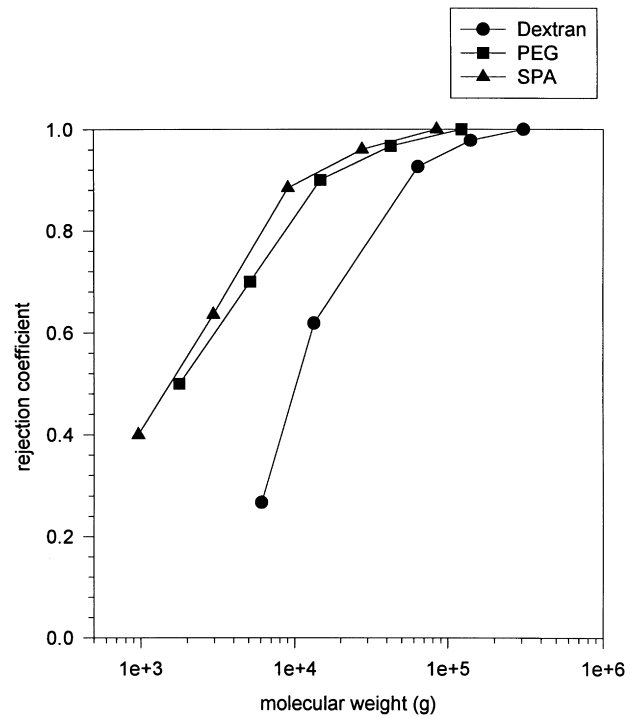


Fig. 4. Rejection coefficients for filtration of dextran, PEG and SPA through asymmetric EVAL membranes at the transmembrane pressure of 0.5 kgf/cm<sup>2</sup>.

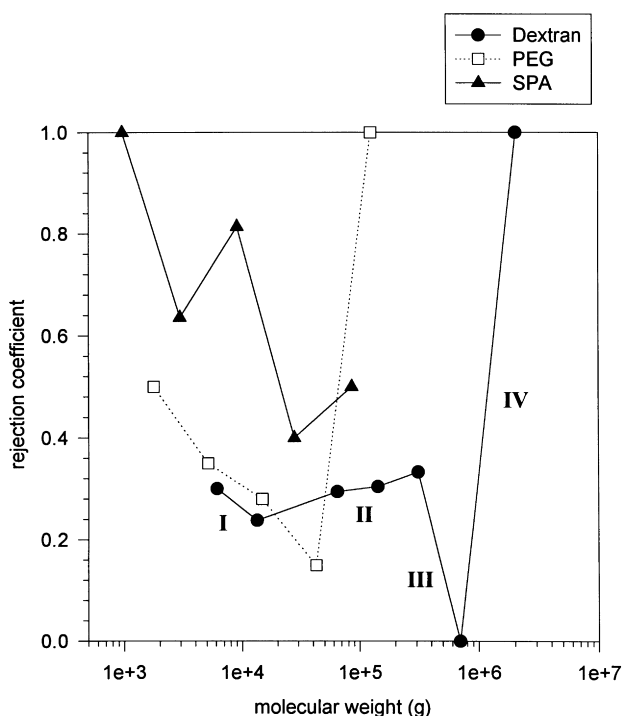


Fig. 5. Rejection coefficients for filtration of dextran, PEG and SPA through particulate EVAL membranes at the transmembrane pressure of 0.5 kgf/cm<sup>2</sup>.

is because the particulate membrane has two types of pores: small pores inside the EVAL particles and large pores surrounding EVAL particles. Therefore, those molecules, which are larger than the small pores, will only transport through the large pores. However, small molecules can transport either through the small or large pores. This leads to the uncommon rejection behavior by particulate membranes. Now, we would like to show with the aid of rejection equations how the dual-pore structure could result into the “W” shape rejection curve shown in Fig. 5. As solute molecules may pass by way of either type of pores,

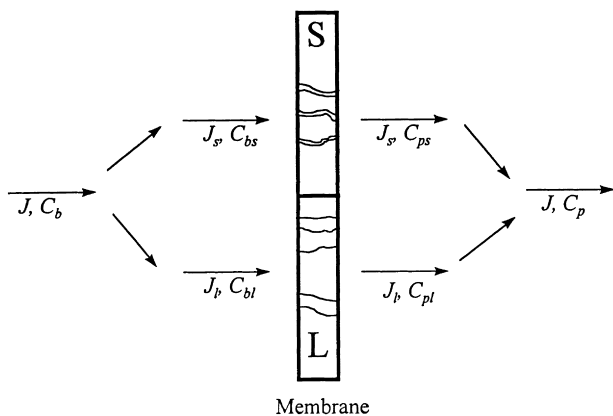


Fig. 6. A parallel composite membrane model for simulating the rejection behavior of particulate membranes. S, a membrane with small pores. L, a membrane with large pores. Other symbols see the text.

the particulate membrane is considered as a composite membrane where one with small channels and the other with large channels stand in parallel, as shown in Fig. 6. Therefore, the concentration of the solute in the bulk ( $C_b$ ) and the permeate ( $C_p$ ) are related to the overall rejection coefficient ( $R$ )

$$R = 1 - \frac{C_p}{C_b}, \tag{1}$$

$$C_b = \frac{1}{J} (J_s C_{bs} + J_l C_{bl}), \tag{2}$$

$$C_p = \frac{1}{J} (J_s C_{ps} + J_l C_{pl}), \tag{3}$$

$$J = J_s + J_l, \tag{4}$$

where  $J$  is total permeate flux, and  $J_s$  and  $J_l$  are the partial flux through the small channels and the large channels, respectively.  $C_{bs}$  and  $C_{bl}$  are the concentrations of solute molecules entering the small pores and large pores, respectively, and  $C_{ps}$  and  $C_{pl}$  are the concentrations of solute molecules that come out of small pores and large pores, respectively. In writing Eqs. (1)–(4), we have, on an average sense, considered the small and the large pores to be two independent and parallel channels; the small channel represents the small pores whereas the large channel represents the large pores. The cases that solute molecules enter small pores followed by large pores or vice versa are lumped into the case of flowing through the small channel, as the resistance for flowing through the large pores are much smaller than that for small pores. The rejection coefficients for small channel,  $R_s$ , and large channel,  $R_l$ , are written, respectively, as

$$R_s = 1 - \frac{C_{ps}}{C_{bs}}, \tag{5}$$

$$R_l = 1 - \frac{C_{pl}}{C_{bl}}, \tag{6}$$

From the definitions of  $R_s$  and  $R_l$  and substitution of Eqs. (2)–(4) into Eq. (1), yields the overall rejection coefficient,

$$R = (1 - k)R_s + kR_l, \tag{7}$$

where  $k$  denotes the ratio of the number of the solute molecules entering large channels to the total number of solute molecules in the feed (i.e.  $k = J_l C_{bl} / J C_b$  and  $1 - k = J_s C_{bs} / J C_b$ ). Eq. (7) suggests that the overall rejection coefficient includes contributions from both types of pores and the proportional constant of the number of solute molecules entering each type of pore.

Now, the rejection coefficients of dextran molecules for particulate membranes are simulated by Eq. (7). For dextran molecules that are far smaller than the large pore (e.g. those in Sections 1 and 2)  $R_l$  is equal to zero because these molecules are small enough to go through the large channels

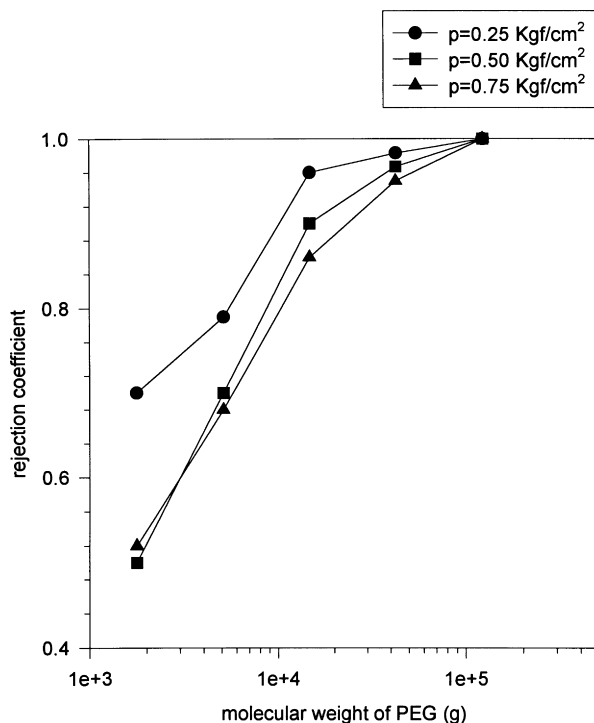


Fig. 7. Rejection coefficients for filtration of PEG through asymmetric EVAL membranes as a function of PEG molecular weight with the applied pressures of 0.25, 0.50 and 0.75 kgf/cm<sup>2</sup>, respectively.

freely. This is justified by the zero rejection occurring at molecular weight equals 700 kDa. As a result, Eq. (7) becomes

$$R = (1 - k)R_s \quad (8)$$

When the molecular weight of dextran is increased, both  $k$  and  $R_s$  are expected to increase. In this event, as indicated in Eq. (8), a competition between  $(1 - k)$  and  $R_s$  arises and the magnitude of the overall rejection coefficient,  $R$ , depends actually on how large these two terms change in response to the increase of molecular weight. If  $(1 - k)$  is more sensitive than  $R_s$ , the overall rejection coefficient will decrease. This is what is observed in Section 1 of the rejection curve. It is reasonable because, in this section, the resistance for transportation is very small (molecular weight of dextran < 10 kDa) and thus,  $R_s$  increases only to a limited extent with molecular weight. In Section 2, the situation reverses; the overall rejection coefficient increases with molecular weight owing to the increasing dominance of  $R_s$ . This is evident from the local maximum rejection at molecular weight equals 300 kDa. In this case the size of dextran molecule approaches that of the small pore, which in turn gives a large  $R_s$ .

In Section 3, complete retention by the small channels occurs for larger dextran molecules, i.e.  $R_s = 1$ . However, in this case, the size of dextrans is still far smaller than the large pores, i.e.  $R_1 = 0$ . Eq. (7) thus becomes

$$R = 1 - k \quad (9)$$

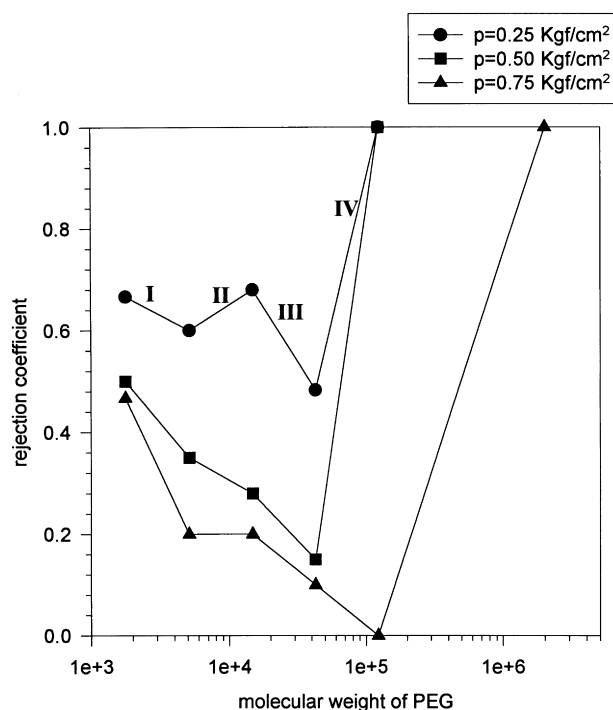


Fig. 8. Rejection coefficients for filtration of PEG through particulate EVAL membranes as a function of PEG molecular weight with the applied pressures of 0.25, 0.50 and 0.75 kgf/cm<sup>2</sup>, respectively.

Eq. (9) indicates that the overall rejection coefficient is decreased when  $k$  is increased as a result of the increasing molecular weight of dextran.

When dextran molecules become larger than the small pores, they are completely excluded from small channels. This corresponds to the case at molecular weight equal to 700 kDa. At this point, the dextran molecules are somewhat larger than the small pores, but much smaller than the large pores. As a result, they transport through large channels with such a little resistance that the overall rejection coefficient approximates zero. For very large dextrans in Section 4,  $R_s = k = 1$ , and Eq. (7) becomes

$$R = R_1 \quad (10)$$

In other words, large dextrans (Section 4) permeate only through the large channels; a typical circumstance for micro- or ultra-filtration. As is anticipated, the rejection coefficient increases with molecular weight, until the point where total rejection occurs.

The rejection curve of SPA through particulate membranes, as shown in Fig. 5, follows the same trend as that of dextran, having the shape of "W". For filtration of PEG at the same pressure, the rejection curve, however, contains only two sections and there exists a minimum at 40 kDa. This may be due to the fact that the PEG molecules are very flexible and thus are subject to significant deformation in the presence of a pressure gradient. In this event, the elongational flux that drives the solutes into the pores of a membrane also stretches the solute molecules so as to

reduce their transverse dimensions, which enables the molecules to pass through much smaller pores than would be possible for less flexible molecules of the same molecular weight. As this phenomenon should be not significant for filtration at a lower transmembrane pressure, the effect of the transmembrane pressure on the membrane performance was studied. Fig. 7 gives the rejection coefficients of PEG through asymmetric membranes as a function of the solute molecular weight, at three different pressures, 0.25, 0.5 and 0.75 kgf/cm<sup>2</sup>. It appears that the retention capability of the asymmetric membranes decreases as the transmembrane pressure is increased. Similar observations have been reported previously for the filtration of dextran through asymmetric membranes [2], and it has been attributed to the fact that the macromolecules are compressed and deformed into configurations that fit easily into the membrane pores at elevated pressures [7,8]. The rejection coefficients for the filtration of PEG through particulate membranes, likewise, decrease with increasing transmembrane pressure, as shown in Fig. 8. However, the rejection curve at low pressure (0.25 kgf/cm<sup>2</sup>) exhibits the four-section characteristic as that shown in Fig. 5 for dextran and SPA at 0.5 kgf/cm<sup>2</sup>. At higher pressures, Sections 2 and 3 disappear, and the rejection curves have only one minimum. Such pressure dependence is also observed in the case of SPA filtration at higher pressures, e.g. 0.75 kgf/cm<sup>2</sup> and larger (not shown here).

#### 4. Conclusion

The separation properties of a membrane depend heavily on the membrane structure. In this work, the rejection coefficients for the permeation of several macromolecular solutes through EVAL membranes have been determined. There are two representative structures for the EVAL membranes, i.e. asymmetric and particulate structures. Although there have been numerous previous studies of large molecules transporting through asymmetric membranes, the particulate membrane has not been extensively studied. The pores of the particulate membrane can

be divided into two categories: small pores in the particles (like small pores in the skin layer of the asymmetric membrane) and large pores between the particles (like large pores in the sublayer of the asymmetric membrane). This porous structure is modeled as an assemblage of two independent and parallel channels; one with small diameter and the other with large diameter corresponding, respectively, to the small and large pores. It follows that the overall rejection coefficient is the sum of contributions from both types of pores. This model illustrates reasonably the unusual “W” shape rejection curves measured for the permeation of macromolecular solutes through the particulate membranes.

#### Acknowledgements

The authors thank the National Science Council of the Republic of China for their financial support of project NSC 86-2216-E-002-003.

#### References

- [1] Loeb S, Sourirajan S. Sea water demineralization by means of an osmotic membrane. *Adv Chem Ser* 1963;38:117.
- [2] Cheng LP, Lin HY, Chen LW, Young TH. Solute rejection of dextran by EVAL membranes with asymmetric and particulate morphologies. *Polymer* 1998;39:2135–42.
- [3] Young TH, Lai JY, Yu WM, Cheng LP. Equilibrium phase behavior of the membrane forming water-DMSO-EVAL copolymer system. *J Membrane Sci* 1997;128:55–65.
- [4] Young TH, Chen LW. A two step mechanism of diffusion controlled ethylene vinyl alcohol membrane formation. *J Membrane Sci* 1991;57:69–81.
- [5] Young TH, Chen LW, Cheng LP. Membranes with a microparticulate morphology. *Polymer* 1996;37:1305–10.
- [6] Bahary WS, Jilani M. Universal calibration assessment in aqueous gel permeation chromatography. *J Appl Polym Sci* 1993;48:1531–8.
- [7] de Balmann H, Nobrega R. Deformation of dextran molecules—causes and consequences in ultrafiltration. *J Membrane Sci* 1989;40:311–27.
- [8] Schock G, Miquel A. Characterization of ultrafiltration membranes: cutoff determination by gel permeation chromatography. *J Membrane Sci* 1989;41:55–67.